

Phase A

**SwissCube
Payload System
Engineering**

DRAFT

Prepared by:
N. Scheidegger

Checked by:

Approved by:

•
Institution
City
Switzerland
•
8/18/2006
•



RECORD OF REVISIONS

| ISS/REV | Date | Modifications | Created/modified by |
|---------|------------|----------------------------------|---------------------|
| 1/0 | 06/25/2006 | | N. Scheidegger |
| 1/1 | 08/09/2006 | Update of the scientific mission | N. Scheidegger |

| | |
|---|-----------|
| RECORD OF REVISIONS..... | 2 |
| FOREWORD..... | 4 |
| INTRODUCTION..... | 4 |
| 1 REFERENCES | 5 |
| 1.1 NORMATIVE REFERENCES | 5 |
| 1.2 INFORMATIVE REFERENCES | 5 |
| 2 TERMS, DEFINITIONS AND ABBREVIATED TERMS..... | 6 |
| 2.1 ABBREVIATED TERMS | 6 |
| 3 DESIGN REQUIREMENTS | 7 |
| 3.1 FREQUENCY OF MEASUREMENTS | 7 |
| 3.2 SPATIAL RESOLUTION | 7 |
| 3.3 SPECTRAL RESOLUTION | 7 |
| 3.4 RESOLUTION OF MEASUREMENTS | 8 |
| 3.5 DYNAMIC RANGE | 8 |
| 3.6 PAYLOAD CONSTRAINTS | 8 |
| 4 DESIGN CONSTRAINTS AND ASSUMPTIONS..... | 8 |
| 5 DESIGN TRADES/ANALYSES | 9 |
| 5.1 LIGHT CONSIDERATIONS | 9 |
| 5.2 SATELLITE ATTITUDE | 10 |
| 5.2.1 <i>Scanning mode</i> | 10 |
| 5.2.2 <i>Coverage</i> | 12 |
| 5.2.3 <i>Pointing accuracy</i> | 14 |
| 5.2.4 <i>Pointing stability</i> | 15 |
| 5.2.5 <i>Horizontal shift</i> | 16 |
| 5.3 SCIENTIFIC INSTRUMENT | 16 |
| 5.3.1 <i>Optical system</i> | 16 |
| 5.3.2 <i>Detector</i> | 19 |
| 5.3.3 <i>Electronic circuit</i> | 21 |
| 5.3.4 <i>Scientific Data</i> | 22 |
| 6 BASELINE DESIGN / ANALYSIS RECOMMENDATIONS..... | 25 |
| 6.1 MASS AND POWER BUDGET OF THE SCIENTIFIC INSTRUMENT | 25 |
| 7 CONCLUSION AND FUTURE WORK | 26 |

FOREWORD

This report presents a preliminary analysis and design of the scientific instrument for the satellite SwissCube. Further design iterations will be necessary until end of Phase A.

INTRODUCTION

The payload mission is to perform space-based observations of the airglow occurring in the upper atmosphere at approximately 100 km altitude. There are both technological and scientific motivations for these measurements. The technological reason hinges on using the nightglow as the basis for a low-cost Earth sensor. By collecting detailed data on the nightglow, the payload will demonstrate (or disprove) the soundness of this Earth sensor concept. The more fundamental reason for the mission is to gain a better understanding of atmospheric physics during the day, principally the intensity of selected oxygen lines, their dependence on latitude, longitude, altitude, solar events and time. There is still a lack of data on fluctuation of airglow intensities and existing models may not be appropriate enough. Finally such a payload would demonstrate the ability of a 1kg satellite to perform a scientifically useful Earth observation mission.

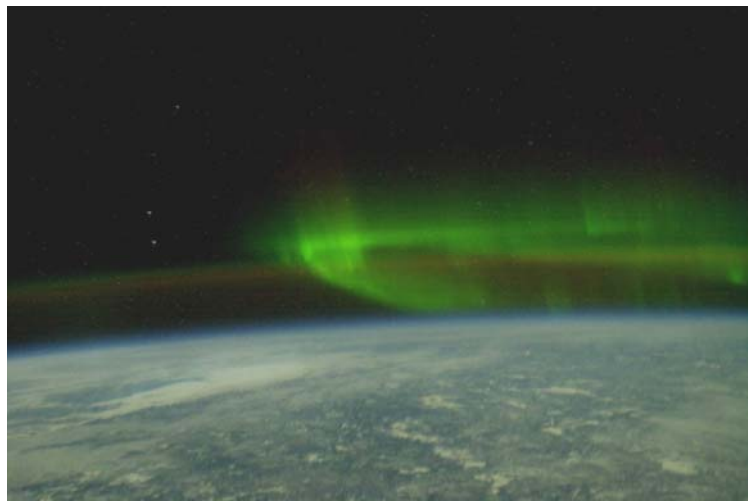


Figure 1: Nightglow and aurora borealis.

1 REFERENCES

1.1 Normative references

1.2 Informative references

- [R1] O. Harang and M.J.Kosch, Absolute Optical Calibrations Using a Simple Tungsten Bulb: Theory, *Sodankylä Geophysical Observatory Publications*, 92:121-123, 2003
- [R2] R. Krpoun and H. Shea, Proposal of payload for EPFL Cubesat: Nightglow limb measurement, EPFL-LMTS, 2005
- [R3] J. Stegman, Department of Meteorology, Stockholm University, private communication
- [R4] R.G.H. Greer, D.P. Murtagh, I.C. McDade, P.H.G. Dickinson, L. Thomas, D.B. Jenkins, J. Stegman, E.J. Llewellyn, G. Witt, D.J. MacKinnon and E.R. Williams, ETON 1: A data base pertinent to the study of energy transfer in the oxygen nightglow. *Planet. Space Sci*, 34: p. 771, 1986
- [R5] A. Foletti; P. Kaewkerd, Phase A – Attitude Determination and Control System. *SwissCube Publications*, Iss 1 Rev. 5, June 2006

2 TERMS, DEFINITIONS AND ABBREVIATED TERMS

2.1 Abbreviated terms

ADCS Attitude Determination and Control System

CCD Charge Coupled Device

d_{limb} Distance between the satellite and the limb

FOV Field Of View

h_{sat} Altitude of the satellite

QE Quantum Efficiency

R Rayleigh

R_E Radius of the Earth

t_{int} Integration time for scientific measurements

SPAD Single Photon Avalanche Diode

Y Vertical resolution of the limb-measurements

X Horizontal resolution of the limb-measurements

3 DESIGN REQUIREMENTS

3.1 Frequency of measurements

Variations in airglow emission intensities are expected to strongly depend on altitude, latitude and local time, especially during day. Hence, these are the driving parameters and determine the frequency measurements. Another important characteristic which has to be analyzed is the stability of the emission with time (dependence of seasonal variations for example). Thus the requirements on the frequency of airglow measurements can be defined as follow:

- Scientific observations shall be made during at least three month. During this period, 20% [TBC] of the Earth's atmosphere shall be covered at night, whereas there shall be at least one dayglow measurement every 10 days [TBC].
- After three month, the nightglow observations will be concentrated on several local regions instead of a global coverage. A specific longitude and latitude shall be measured at the same local time of measurements within 10 days [TBC]. The local time of measurements shall not vary more than 10 minutes [TBC]. An observation of oxygen emissions over one year would allow analyzing seasonal variations.
- The position of the satellite during measurements shall be determined with a precision of 5° (3σ) for longitude and 2° (3σ) for latitude [TBC]. The orientation of the satellite shall be determined with an precision of 3° (3σ) for every angle [TBC].

3.2 Spatial Resolution

In order to provide significant measurements for a detailed map of the airglow in the upper atmosphere, the area of interest (between 80 and 110 km altitude) should be captured with a vertical resolution of 5 km. Since we use square pixels, the effective input area per pixel has to be $3.5 \text{ km} \times 3.5 \text{ km}^1$ to guarantee a resolution of at least 5 km regardless of the satellite's orientation. The horizontal resolution is less important, since we expect only a moderate rate of the airglow emission for a given altitude. A horizontal resolution of 200 km would be sufficient. It will be defined by the integration time (see chapter 5.2.4) and the pixel size of the detector.

3.3 Spectral Resolution

The only airglow line which requires a narrow filtering is the 762 nm A-Band molecular oxygen line. For this wavelength, the spectral resolution has to be around 5 nm (3σ) to guarantee a proper selection of the $\text{O}_2\text{A}(0-0)$ oxygen line.

¹ Thus the pixel diagonal is 5 km.

3.4 Resolution of Measurements

The resolution of the measurements is defined as the smallest variation in emission intensity which can be detected. It depends on the incident photon flux per pixel and the SNR. The resolution shall be at least 5 % [TBC] (1σ) of the mean incident photon flux on the detector which was emitted by an area of 3.5 km x 3.5 km at the limb.

3.5 Dynamic Range

The minimum and maximum number of photons which can be measured by a pixel is 16 [TBC], respectively 1024 [TBC]. Hence the dynamic range of the measurements is 36 dB[TBC].

3.6 Payload Constraints

The whole scientific instrument has to fit in a volume of 50 x 50 x 90 mm³ and weight less than 100g. The power consumption should be minimized as much as possible since the payload will also operate during eclipse times. A power consumption of less than 25 mWh is required.

4 DESIGN CONSTRAINTS AND ASSUMPTIONS

Several constraints and assumptions had to be made for the analyses described in chapter 5. To simplify the lecture of this report, they are repeated in the sections where they are used for calculations. Nevertheless they are summarized below.

- [A1] The altitude of the satellite ranges between 400 km and 1000 km. The scientific instrument has to be able to operate efficiently for any satellite altitude within this range.
- [A2] The average contact time period between the satellite and a ground station is 10 minutes per day, whereof 5 minutes can be used for the transmission of scientific data.
- [A3] A compressed image has a size of 5 kbits whereas an uncompressed image needs 180 kbits.
- [A4] The Earth's coverage is complete if the atmosphere between a latitude of - 80° and + 80° is covered.
- [A5] The depth of the measurements of the limb is around 500 km.
- [A6] The satellite does 14 orbits in one day.
- [A7] The image stability must remain below 30 % for an input area of 3.5 km x 3.5 km.
- [A8] The F-number of the optical lenses shall not be smaller than 1.
- [A9] The SNR of the scientific measurements shall be at least 20.

5 DESIGN TRADES/ANALYSES

5.1 Light considerations

Nightglow measurements from space have been made by the Imaging Spectrometric Observatory (ISO) on the Shuttle during the Atlas-1 mission and by the Arizona Airglow Experiment on STS-69. The most prominent feature visible from ground is the 557.7 nm atomic oxygen O(¹S) green line, whereas the strongest nightglow band, only visible from space, is the O₂A(0-0) at 762 nm.

The 762 nm A-Band molecular oxygen line is measurable at day and night sky. The dayglow measurements can give information about the ozone profile between 80 and 110 km and the temperature climatology for mesopause region if taken with a resolution of 0.5 nm.

A measurement of the atom O(¹S) in line 557.7 nm could be used for calibration in combination of ground based observation of the same line.

Table 1 gives the limb emission rates² of the different wavelengths at an altitude of 100 km.

| | Nightglow [Rayleigh] | Dayglow [Rayleigh] |
|-------------------------------|----------------------|--------------------|
| 557.7 nm O ₂ (0-1) | 8'000 | 240'000 |
| 762 nm O ₂ (0-0) | 400'000 | 24'000'000 |

Table 1: Emission rates of the different wavelengths at the limb.

According to [R1], the system response per Rayleigh can be calculated with the formula

$$res = \frac{1}{4\pi} 10^{10} \cdot S \omega \quad [\text{photons R}^{-1} \text{ s}^{-1}]$$

Where S is the input area [m²] and ω is the solid acceptance angle [sr].

For a satellite altitude $h_{sat} = 400$ km, a limb altitude of $h_{limb} = 100$ km and an area of observation A of 3.5 km x 3.5 km per pixel, the solid angle is

$$\omega = \frac{A}{(R_E + h_{sat})^2 - (R_E + h_{limb})^2} = \frac{3.5 \cdot 3.5}{(6378 + 400)^2 - (6378 + 100)^2} = 3.08 \cdot 10^{-6} [\text{sr}]$$

For an input area $S = 5 \text{ cm}^2$ (telescope with an aperture of $\varnothing 25$ mm), the photon flux per Rayleigh onto a pixel of the detector is then

$$res = \frac{1}{4\pi} 10^{10} \cdot S \omega = \frac{1}{4\pi} 10^{10} \cdot 5 \cdot 10^{-4} \cdot 3.08 \cdot 10^{-6} = 1.23 [\text{photons}/(\text{R} \cdot \text{s})]$$

² These emission rates are valid for limb measurements only and based on [R3] and [R4].

Table 2 and Table 3 give the incident photon flux onto a pixel of the detector for the different wavelengths and different altitudes. It is important to remember that these values are valid for a resolution of 3.5 km x 3.5 km per pixel and a telescope aperture of Ø25 mm.

| | Nightglow [photons s ⁻¹ pixel ⁻¹] | Dayglow [photons s ⁻¹ pixel ⁻¹] |
|-------------------------------|--|--|
| 557.7 nm O ₂ (0-1) | 10 k | 295 k |
| 762 nm O ₂ (0-0) | 490 k | 29.5 M |

Table 2: Incident photon flux per pixel for a satellite altitude of 400 km.

| | Nightglow [photons s ⁻¹ pixel ⁻¹] | Dayglow [photons s ⁻¹ pixel ⁻¹] |
|-------------------------------|--|--|
| 557.7 nm O ₂ (0-1) | 3 k | 93.6 k |
| 762 nm O ₂ (0-0) | 155 k | 9.36 M |

Table 3: Incident photon flux per pixel for a satellite altitude of 1000 km.

5.2 Satellite attitude

5.2.1 Scanning mode

There are two interesting operation modes for the scanning of the Earth's limb:

The first scanning mode, the spin-mode, consists of rolling the telescope's FOV across the limb as shown in Figure 2. Theoretically, the satellite's attitude will not need to be controlled precisely as long as the FOV scans between staring at space, passing through the limb, staring at Earth, passing a second time through the limb and staring at space again in a few minutes. However, the spacecrafts spin rate has to be very low to provide a sufficient pointing stability during the measurements of the limb (see section 5.2.4). The main drawback of this scanning mode is the fact that it is very difficult for the attitude control (ADCS) to ensure such a constant low spin rate for a small satellite. Furthermore, it will be difficult to reconstruct a map of the nightglow, since two successive measurements do not correspond to neighboring regions of the limb.

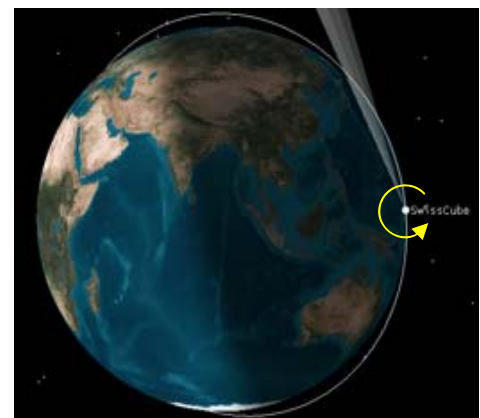


Figure 2: Spin-mode

In the second operation mode for measuring the airglow, called the side-looking-mode, the satellite will always point at the limb (Figure 3). An area of at least 30 km x 100 km (see chapter 3.2) will be captured in a single frame by a detector array. The main advantage of this operation mode is the simplification of the attitude control since there is no active scanning of the limb. Instead of a constant spinning attitude, the satellite will be stabilized which is much easier to control.

Furthermore, the reconstruction of the airglow map will be simpler, since two successive images will correspond to two neighboring regions of the atmosphere (Figure 4) for one half orbit³. Another important factor is the fact that for nightglow measurements the local time of measurements is expected to be around midnight with the side-looking-mode, allowing thus to observe zones of weak oxygen emission. These zones have a big impact on the feasibility of using the nightglow as the basis for a low-cost Earth sensor and are therefore of great importance.

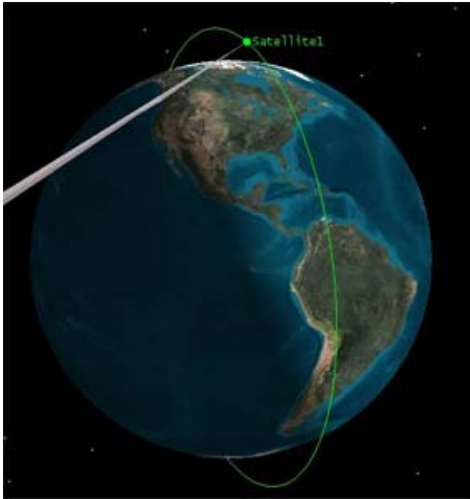


Figure 3: Side-looking-mode

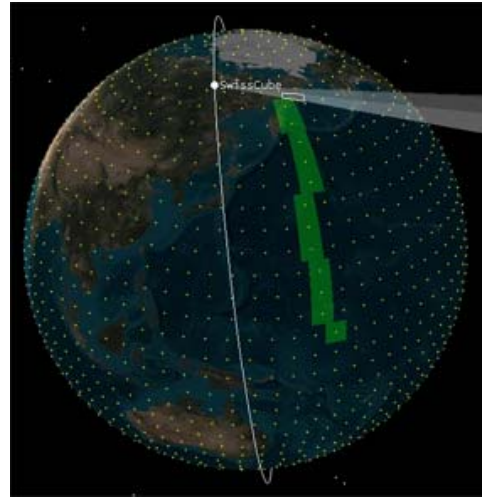


Figure 4: Coverage of the Earth's atmosphere in stripes with the side-looking-mode.

The third scanning mode, called back-looking-mode, is similar to the second one: the satellite is stabilized and always points at the limb. Instead of looking on the side, it will point the limb in its orbit plane as shown in Figure 5. For ADCS this scanning mode is the easiest to control, since it is passively stabilized by the momentum wheel⁴. The first drawback of this solution is the reconstruction of the airglow map, which will be more difficult since two successive images will not correspond to neighbouring regions. A second drawback is the fact that zones the local time of measurements will be around 9 p.m. where more intense nightglow will be observed. Hence, the zones of weaker emission affecting the feasibility of the low-cost Earth sensor will not be measured.

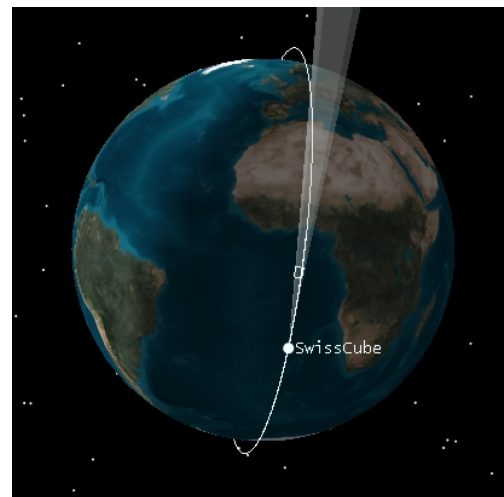


Figure 5: back-looking-mode

³ Airglow will be measured in continuous over a half orbit during either eclipse or sunlight times.

⁴ For further details see [R5].

5.2.2 Coverage

To observe the dependence of night- and dayglow on latitude, longitude, altitude, solar events and time, scientific measurements have to be made as frequently as possible. The percentage of the Earth's atmosphere which will be covered by the measurements is limited by the data downlink and the available power.

As described in the previous section, the airglow will be measured in continuous over half an orbit during eclipse time and half an orbit during sunlight time. For a complete coverage of a stripe between -80° and $+80^\circ$ latitude, we need

$$\frac{2\pi \cdot (R_E + h_{\text{limb}}) [\text{km}] \cdot 160 [^\circ / \text{orbit}]}{360 [^\circ]} \cdot \frac{1}{500 [\text{km} / \text{image}]} = 36 [\text{image} / \text{stripe}]$$

Where $R_E = 6378$ km is the Earth's radius and $h_{\text{limb}} = 100$ km is the limb altitude.

Assuming that a processed image has a size of 5 kbit we have to store

$$36 [\text{images} / \text{orbit}] \cdot 5 [\text{kbit} / \text{image}] = 180 [\text{kbit} / \text{stripe}]$$

If we assume further an average access time of 10 minutes per ground station, we should be able to transfer scientific data during 4 minutes ([A2]). With a data rate of 1.2 kbps we would have

$$4 [\text{min} / \text{access}] \cdot 60 [\text{s} / \text{min}] \cdot 1.2 [\text{kbps}] = 288 [\text{kbit} / \text{access}]$$

For the transfer of the measurements of an orbit, we would need

$$\frac{180 [\text{kbit} / \text{stripe}]}{288 [\text{kbits} / \text{access}]} = 0.625 [\text{access} / \text{stripe}]$$

To transmit scientific data of one complete stripe during either eclipse times or sunlight times it would therefore require 1 access. If we add a supplemental access as margin, we need two accesses to transmit scientific data of one stripe.

If a cycle repetition shall be performed in m days, the percentage of coverage of the Earth's atmosphere can be calculated according to the equation

$$\frac{n [\text{access} / \text{day}] \cdot m [\text{days}]}{2 [\text{access} / \text{stripe}]} \cdot \frac{450 [\text{km} / \text{orbit}]}{2\pi \cdot (R_E + h_{\text{limb}}) [\text{km}]} = n \cdot m \cdot 0.0055 []$$

Where n is the numbers of ground stations which receive data from the satellite.

Figure 6 shows the percentage of coverage of the Earth's atmosphere between a latitude of -80° and $+80^\circ$ at night depending on the number of ground stations which will communicate with the satellite and the time when the coverage is fulfilled (cycle repetition of the measurement). A complete coverage would require three ground stations and a cycle repetition of 60 days or two ground stations and a cycle repetition of 90 days. With a cycle repetition of the measurements of 10 days as required by the science mission, 15% of the Earth's atmosphere at night could be covered with three ground stations.

It is important to notice that the calculated values give the maximum theoretical coverage of the Earth's atmosphere. Parameters such as the satellite ground track repetition cycle which might inhibit a complete coverage of the Earth's atmosphere have not been taken into consideration. Further mission analyses have to be made to give the effective values for the coverage.

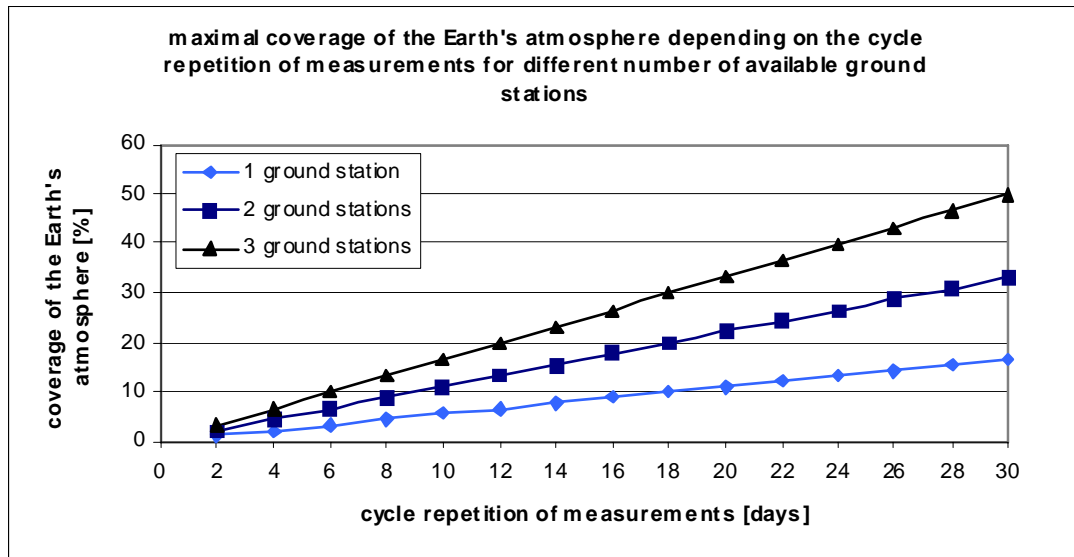


Figure 6: Percentage of coverage of the Earth's atmosphere in function of the number of available ground stations for different cycle repetition of the measurements corresponding to a specific longitude, latitude and local time.

Another important characteristic is the frequency of scientific measurements. Since we need 2 accesses to transfer the measurements of one orbit we can measure at maximum

$$\frac{n [\text{access/day}]}{2 [\text{access/stripe}]} = \frac{n}{2} [\text{stripe/day}]$$

Thus, if the satellite does 14 orbits in one day [A6] and since measurements are done over half an orbit (during either eclipse times or daylight times), we will do scientific observations each

$$\frac{14 \cdot 2}{n} [\text{orbit}]$$

Figure 7 shows the number of orbits between two orbits where scientific measurements are taken. If there was one single ground station communicating with the satellite, scientific observations could be made each 28th orbit only. To guarantee a reasonable frequency several ground stations are required. However, the frequency of measurements is limited by the available power for a high number of disposable ground stations. Hence, scientific observations can be made each 3rd orbit at maximum due to power limitation.

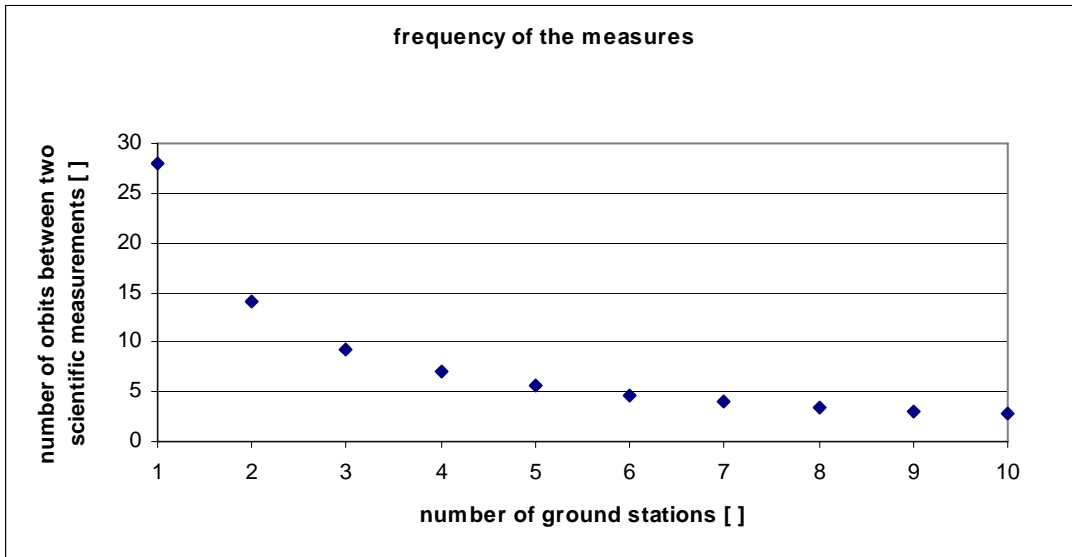


Figure 7: Frequency of scientific measurements.

5.2.3 Pointing accuracy

For a side-looking scanning mode the required pointing accuracy α (3σ) in roll depends on the altitude of the satellite and the size of the detector-array. As mentioned in section 0, airglow occurs in a vertical zone of 30 km and should be measured with a spatial resolution Y of 3.5 km. To guarantee that the whole zone of interest (9 pixels) is captured by the detector-array it has to be equal or bigger than

$$n = 2 \cdot \frac{\tan\left(\frac{\alpha}{2}\right) \cdot d_{\text{limb}}}{Y} + 9 = 2 \cdot \frac{\tan\left(\frac{\alpha}{2}\right) \cdot \sqrt{(R_E + h_{\text{sat}})^2 - (R_E + h_{\text{limb}})^2}}{Y} + 9 \quad []$$

Where n is the number of pixels (for a resolution of 3.5 km per pixel)

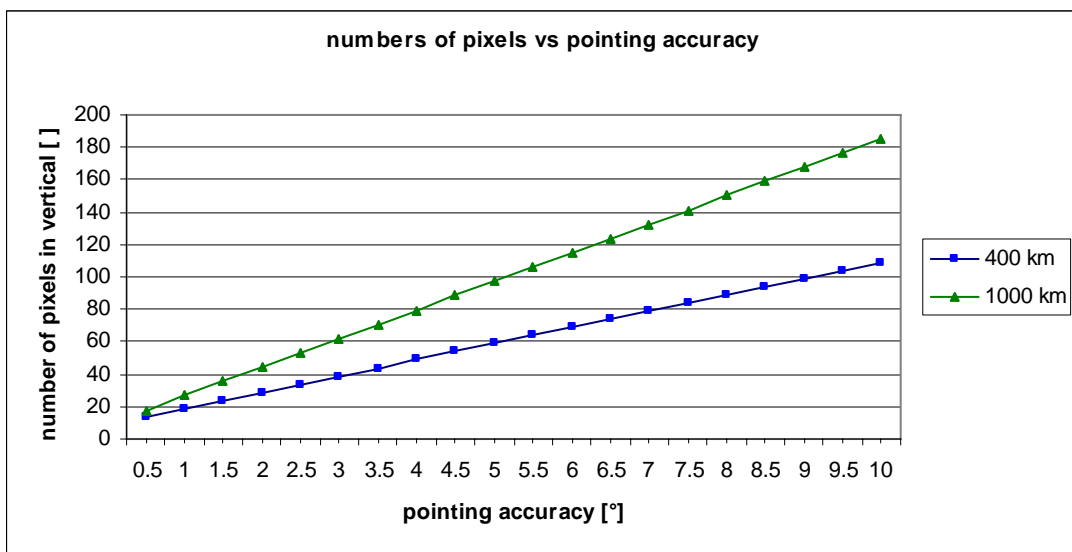


Figure 6: Required detector size in function of the provided pointing accuracy.

As shown in Figure 6 a detector size of 128 pixels x 128 pixels will be sufficient to ensure that the airglow emission will be captured when pointing the limb with an accuracy (3σ) of 6.5° at a satellite altitude lower than 1000 km. The requirement for the pointing in both other angles (yaw and pitch) is fairly relaxed since the image is reasonably insensitive to its variations. It will however affect the local time of the tangent point.

5.2.4 Pointing stability

The pointing stability $\Delta\alpha$ in roll and pitch⁵ has a big impact on the correctness of the image. In order to give significant measurements, the photons emitted from the input area of one pixel should not shift more than 30%. The minimal required pointing stability for a certain integration time can be calculated with the formula:

$$\Delta\alpha = O = \frac{Ov \cdot FOV_{pixel}}{t_{int}} = \frac{Ov \cdot \sin^{-1}\left(\frac{Y}{d_{limb}}\right)}{t_{int}} \quad [^\circ/s]$$

Where $Ov = 0.3$ is the shifting of the input area, called overlapping, FOV_{pixel} is the field of view of a single pixel, $Y = 3.5$ km is the vertical spatial resolution, d_{limb} is the distance between the satellite and the limb and t_{int} is the integration time during which the image is taken.

Figure 9 shows that for a high integration time, the required pointing stability required decreases exponentially. The stabilization of the satellite during the measurements is therefore of prime importance. On one hand the integration time should be as small as possible to relax the requirements on pointing stability. On the other hand, the time to measure the incident photons should be as high as possible to increase the SNR. To assure a SNR of 20 when measuring nightglow emission with a satellite altitude of 1000km, an integration time of 0.17 s and a pointing stability of $0.1^\circ/s$ are required for a SPAD-array (see section 5.3.2).

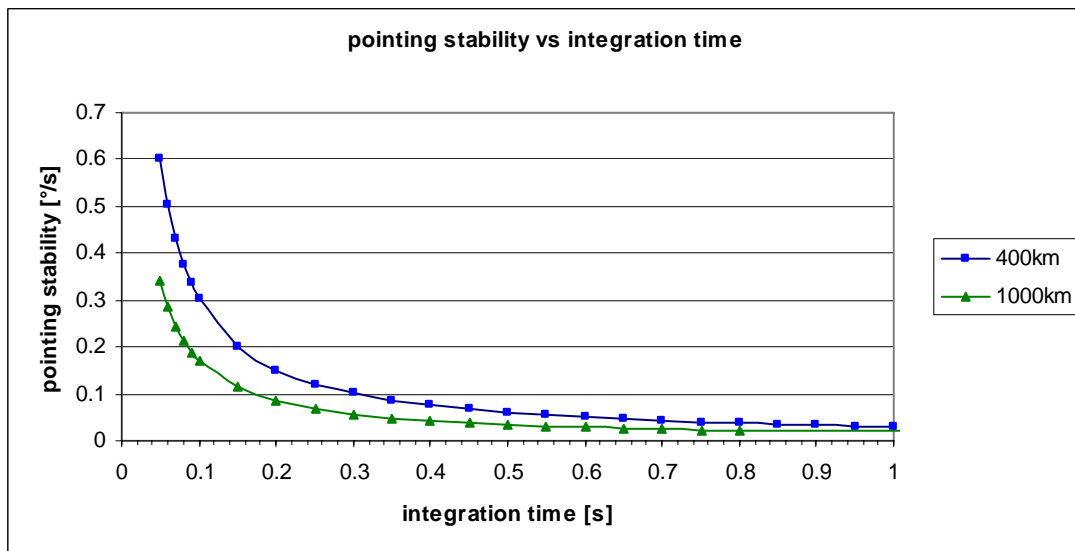


Figure 7: Pointing stability as a function of integration time for 400 km and 1000 km altitude.

⁵ The requirement for the pointing stability in yaw angle is relaxed since the image is insensitive to its variations.

5.2.5 Horizontal shift

Another error in the measurements is due to the movement of the satellite. The displacement of the satellite during the measure results in a horizontal shift of the image which can be calculated according to the following formula.

$$v_{image} = \frac{2\pi \cdot r_{//}}{P_{sat}} \quad \text{where} \quad r_{//} = r_{limb} \cdot \left(\sin \frac{\pi}{2} - \alpha \right) \quad \text{and} \quad \alpha = \cos^{-1} \left(\frac{r_{limb}}{R_E + h_{sat}} \right)$$

With P_{sat} = period of the satellite's orbit and $r_{limb} = R_E + h_{limb}$

This gives an image velocity of

- 7 km/s if the satellite is at an altitude of 400 km and
- 5.7 km/s if the satellite is at an altitude of 1000 km.

The horizontal shift is given by

$$\Delta X = v_{image} \cdot t_{int} \quad [\text{km}]$$

For an integration time of $t_{int} = 0.05$ s at an altitude of 400 km and $t_{int} = 0.17$ s at an altitude of 1000km, the horizontal shift due to the satellite's displacement during the integration time is

- 2 0.35 km if the satellite has an altitude of 400 km and
- 3 0.969 km if the satellite has an altitude of 1000 km.

Since in both cases the overlapping due to the orbital movement of the satellite is smaller than 30%, no correction will be needed for the horizontal pointing during the measurement.

5.3 Scientific Instrument

The payload consists of three main elements:

- an optical system used to image a selected line of the airglow on a detector
- a detector which detects incoming photons and generates an output proportional to the local light intensity
- an electronic circuit which provides the required power and control signals for the detector, reads its output, performs data analysis and compression and interfaces with the satellite bus.

5.3.1 Optical system

The payload's optical system is characterized by its aperture, its focal length and the size of the image of an area of 3.5 km x 3.5 km which are linked through the following formulas:

$$F - \text{number} = \frac{f}{D} \geq 1$$

$$\frac{f}{d_{limb}} = \frac{q}{Y}$$

Where f is the focal length⁶, D is the aperture and q is the size of the image on the detector.

⁶ The distance d_{limb} is very high compared to the telescope size, thus the focal and image plane are used interchangeably.

These two relationships show the trade-off which has to be made: On one hand, the telescope aperture D has to be as large as possible in order to achieve a maximal signal-to-noise-ratio, hence capturing enough photons per second and pixel. On the other hand, the focal length of the telescope should be reduced as much as possible to minimize the exterior dimensions of the optical system and to project the image of the airglow on a smaller detector array. Two optical concepts were considered:

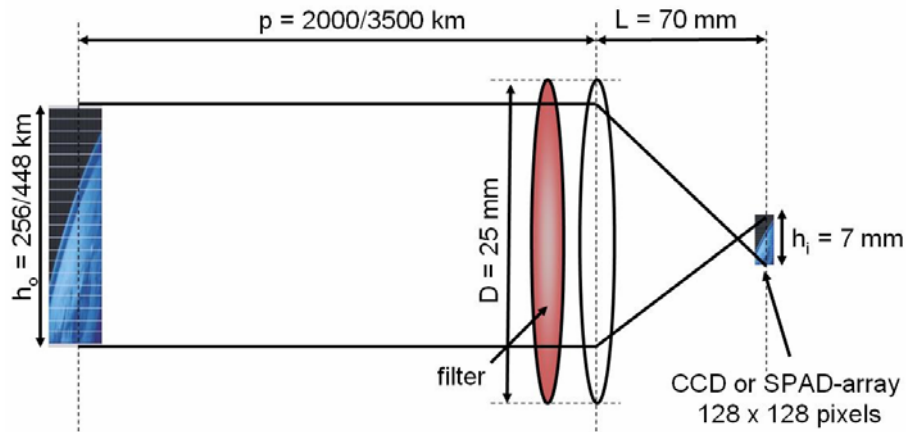


Figure 10: Optical system with 1 lens only.

The first system comprises one lens only (Figure 10). For a satellite altitude of 1000 km, an area of 3.5 km x 3.5 km is projected onto a single pixel. Thus, the resolution Y of the image will be better for a lower satellite altitude as shown in Figure 11. The main advantages of this solution are its simplicity.

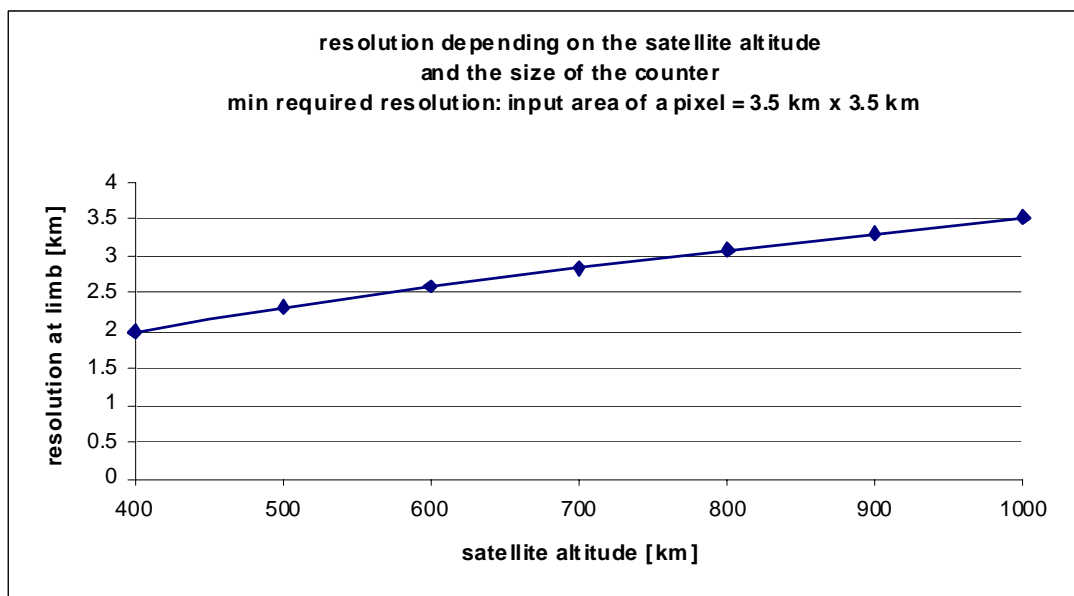


Figure 11: Variation of the resolution of the measurements at limb depending on the satellite altitude.

The second system is a cascade of two lenses as shown in Figure 12. As for the previous version the telescope projects an area of 3.5 km x 3.5 km on a single pixel, but with a reduced overall length of the optical system. The distance L between the first lens and the focus plane can be calculated according to the equation:

$$L = \frac{d - f}{\frac{d}{f} - 2} [\text{mm}]$$

Where d is the distance between the two lenses.

Hence, the scientific instrument will be shorter if two lenses are used. The main drawback of the second solution is its complexity introduced by the second lens.

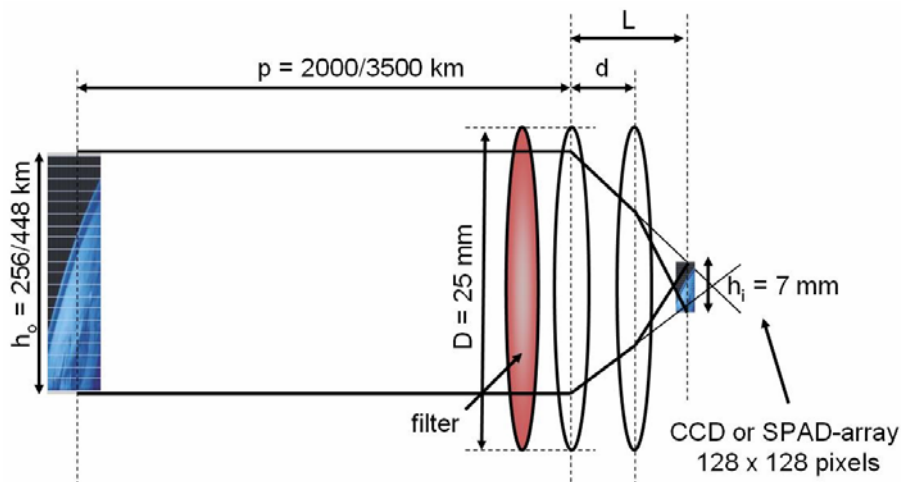


Figure 12: Optical system with 2 lenses.

| | | |
|---|--|--|
| Option | 1 lens: D = 25 mm, f = 65 mm | 2 lenses: D1 = D2 = 25 mm, f1 = f2 = 65 mm |
| Max. exterior dimensions (without electronics) | Ø30mm x 70 mm | Ø30mm x 35 mm (assuming a distance of 10 mm between the two lenses) |
| Image size on detector | 7 mm = 128 pixels | 7 mm = 128 pixels |
| Image resolution (@ 400/1000km) | 2/3.5 km (optics has to be designed for a satellite altitude of 1000 km) | 2/3.5 km (optics has to be designed for a satellite altitude of 1000 km) |
| Mass of the lense(s) | 20g | 40g |
| Mass of the support | 100g | 50g |
| Mass of the electronics | 10g | 10g |
| Total mass | 130g | 100g |
| Onboard processing | Compression of a image with 128x128 pixels and 11bits/pixel to an image with ~5kbits/image | Compression of a image with 128x128 pixels and 11bits/pixel to an image with ~5kbits/image |

Table 4: Characterization of the different optical systems

Table 5 shows the evaluation criteria between the two concepts. Both solutions are not satisfying and an optimization of the optical system is required. Nevertheless, the system with two lenses seems to be the more promising solutions due to it's reduced mass and dimensions.

| Option | Factor of importance | 1 lens: | 2 lenses: |
|------------|----------------------|---------|-----------|
| Simplicity | 1 | + | - |
| Dimensions | 2 | - | + |
| Mass | 3 | - | - |
| Total | | ---- | -- |

Table 5: Evaluation of the different optical systems.

5.3.2 Detector

There are several very mature and high-performance technologies for detecting radiation in the visible to near IR band. The most interesting technologies for our application are Charge Coupled Devices (CCD) and Single Photon Avalanche Diodes (SPAD). Both image sensors can be obtained in a focal plane array configuration. The incoming photons generate electron-hole pairs proportional to the local illumination intensity.

In a CCD sensor, every pixel's charge is transferred through an output node to be converted to voltage (charge-to-voltage converter), buffered and sent off-chip as analog signal. Since there is no on-pixel processing, the complete area of each pixel can be used to capture light (fill factor of 100%) and the output's uniformity is high. All pixels must be read at once. The main drawback of a CCD detector is its performance limitation in low-light situations because each incoming photon generates at most 1 electron. Combined with a high Dark Current, they are not efficient to measure single photons (see Table 6).

A SPAD is a p-n junction biased a few volts above breakdown voltage. A primary carrier resulting from the absorption of a photon can generate an infinite number of secondary electron-hole pairs by impact ionization. SPADs allow very weak optical signals to be detected, with a noise level of only 1 Hz. Compared to CCDs, they have a much higher dynamic range, allowing SPADs to image in bright conditions as well. The main drawbacks are low fill-factor and lower pixel count.

The characteristics of each technology are summarized in Table 6. The photon flux and the SNR have been calculated for the worst case, hence for

- the airglow emission of the 762 nm line,
- a satellite altitude of 1000 km (which corresponds to the worst case in sense of oxygen emission intensities),
- a telescope aperture of 25 mm,
- a resolution of 3.5 km x 3.5 km per pixel and
- a SNR of 20.

| Performance | Unit | CCD | SPAD |
|---|---|-------------------------|-------------------------|
| Max. dynamic range | dB | 80 | 120 |
| Max. fill-factor | % | 100 | 15 |
| Minimum signal | photons | 1000 | 1 |
| Dark Counts (20°) = shot noise | Hz | 2000 | 1 |
| Read-out noise | rms | 9 | 0 |
| Read-out modes | | Flash, sliding, shutter | Flash, sliding, shutter |
| Integration time | μs | 1-1000 | > 0.03 |
| Quantum Efficiency | % | 60 | 10 |
| Mean photon flux at night (including fill factor and QE) | photons pixel ⁻¹ s ⁻¹ | 93'600 | 2'340 |
| Mean photon flux at day (including fill factor and QE) | photons pixel ⁻¹ s ⁻¹ | 5'616'000 | 140'400 |
| Max. required integration time | s | 0.004 | 0.17 |

Table 6: Characterization of the different detector types.

The CCD-array seems to be the most promising solution due to its high fill-factor and quantum efficiency. Nevertheless, SPADs might be used for the satellite, since this would allow using a novel lower cost solution developed at EPFL.

5.3.2.1 Signal-to-Noise-Ratio

The signal-to-noise-ratio of both detectors (CCD and SPAD) can be calculated according to the formula

$$SNR_{pixel} = \frac{QE \cdot p \cdot t_{int}}{\sqrt{(QE \cdot p + SN) \cdot t_{int} + SR}} \quad [\text{photons}^{1/2}]$$

Where QE is the quantum efficiency of the detector depending on the wavelength of the measured photons, p are the incident photons per second on a single pixel, t_{int} is the integration time, SN is the shot noise and SR is the read-out noise of the detector.

The signal-to-noise-ratio of the detector can be improved by binning. By reading the values of n x n pixels as a single value, the SNR of the binning is given by

$$SNR = n^2 \cdot SNR_{pixel} \quad []$$

5.3.3 Electronic circuit

The electronic circuit of the payload will comprise

- the detector,
- a temporary memory where the uncompressed image coming from the detector is stored and treated,
- a micro-processor which does the image compression
- a data bus which links the micro-processor with a second memory, where scientific data is stored until they are transmitted to the ground station.

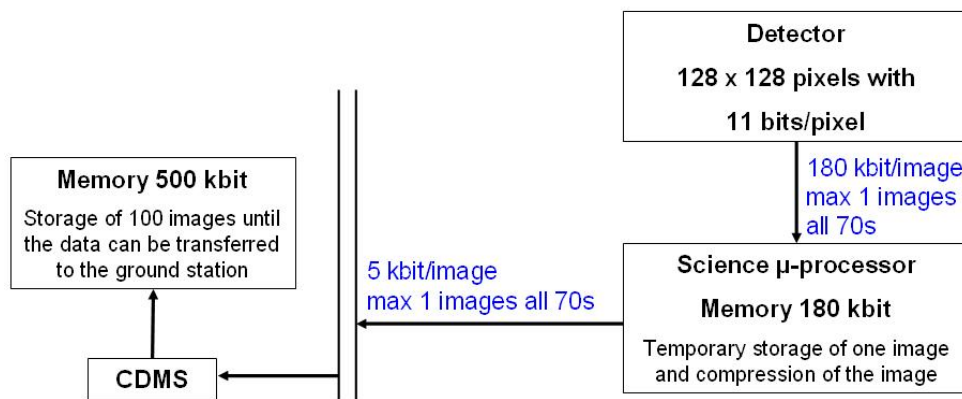


Figure 8: Data transfer on the satellite.

As calculated in subsection 5.2.2 we will have to store about 180 kbit of scientific data until we can transfer it to a ground station. Hence, we should have around 500 kbit of memory for long-term storage. Furthermore, there will be a “temporary” memory of at least 180 kbit where the uncompressed data coming from the detector will be stored and treated.

To guarantee a continuous coverage of the Earth’s limb over half an orbit, the frequency of capturing an image has to be (see subsection 5.2.5 for the calculation of the velocity of the image v_{image})

$$f_{image} = \frac{v_{image}}{X_{image}} = \frac{v_{image}}{500km} = 0.014Hz \text{ for } h_{sat} = 400km \quad \text{and} \quad 0.011Hz \text{ for } h_{sat} = 1000km$$

Thus, we have at least 71 s to capture an image, transfer it to the “temporary” memory, compress the image with the “scientific μ -processor” in the “temporary” memory and transfer it to the “long-term” memory. It is important to notice that there has to be a fast access rate between the “temporary” memory and the “scientific μ -processor”, whereas it can be much lower between the “long-term” memory and the “scientific μ -processor”.

5.3.4 Scientific Data

The scientific data can be separated in three types of data

- the raw data, read directly from the detector and stored immediately in the “temporary” memory
- the compressed data, stored in the “long-term” memory and sent to the ground station
- the header which gives information about the parameters of the image and is stored and transmitted with it’s corresponding image

5.3.4.1 Raw data

The data output of the detector is immediately compressed by storing only the bits needed to provide the required precision of measurements [TBC]. Thus, the raw image is represented by 256 gray levels (8 bits per pixel) corresponding to the intensity of emission and has a size of 130 kbits [TBC]. To reduce the image to a size of 5 kbits, the image has to be compressed by a factor of 26.

5.3.4.2 Compression algorithm

Data compression is used to reduce the volume of digital data to achieve benefits in areas including

- reduction of transmission channel bandwidth
- reduction of the buffering and storage requirement
- reduction of data-transmission time at a given rate

A data compression algorithm is characterized by its compression efficiency, its complexity and hence the required time to execute. Usually, more complex algorithms yield greater data reduction and take longer time to execute. The compression algorithm used to reduce the scientific data on SwissCube has to satisfy the following requirements:

- [RC1] the compression guarantees the required precision of measurements
- [RC2] one image does not depend on the previous images
- [RC3] each image begins and ends with a header which indicates when the image has been taken
- [RC4] the size of the compressed image is smaller than 5 kbits [TBC]
- [RC5] the required time for compression is below 50 s [TBC]
- [RC6] the microcontroller used for the compression consumes less than 25 mWh [TBC]

Furthermore, it would be advantageous to have a robust compression which is able to handle single bit errors.

The algorithm used for image compression has to be chosen carefully. A trade-off has to be made between the compression efficiency, its complexity and the losses introduced by the compression algorithm. Several compression techniques might be interesting for SwissCube:

a) Choosing only the pixels which have a value > threshold

The threshold compression is a lossy data compression which consists in selecting and transmitting only those pixels receiving nightglow intensities above a specified intensity. Such data processing can reduce the data rate by a factor of 5, but extra bits have to be inserted to identify the position of the pixels in the scan. Furthermore, the threshold of the intensities to be transmitted has to be chosen carefully in order to exclude (if desired) the airglow emission which is not emitted from the limb.

b) Shannon-Fano Coding

The basic idea behind of Shannon-Fano coding is using variable length of bits to encode the source symbols according to their absolute frequency. The more frequent the appearance of a symbol, the shorter the code length. It is important to notice that a dictionary has to be stored and sent along with the compressed data if the dictionary is updated for each frame. Furthermore, there has to be free memory of 8 x 8 bits aboard the satellite to store the frequency of each value. The Shannon-Fano coding is a promises no data loss. The main drawback of the Shannon-Fano method is the fact that it is not optimal since it sometimes assigns a longer code to a more probable source symbol than it does to a less probable one, leading to a longer average code length.

c) Huffman's algorithm

Huffman's algorithm takes as input a list of probabilities associated with the source letters and constructs a full binary tree whose leaves are labeled with the weights. It is the coding technique that produces the shortest possible average code length given the source symbol set and associated probabilities. A memory of 8 x 8 bits is required aboard the satellite to store the probability of each of the 256 possible values of emission intensity, whereby the list of probability can be periodically updated. After each actualization of the list of probabilities it has to be stored and sent along with the image. The Huffman's algorithm is a lossless data compression algorithm. Although Huffman coding is efficient, it is optimal only if the probability distribution of a source is known and each source symbol is encoded in integral number of bits. In practice, a Huffman coding is developed on a set of images, but is then applied to many other images, each of which has its own probability distribution of symbols. Thus, the Huffman coding is not necessarily optimal for any particular image.

d) JPEG

JPEG is a well known compression algorithm to reduce the storage and/or transmission cost for image. Compressed images can be interchanged among different applications. The JPEG baseline algorithm is a DCT (discrete cosine transform) based compression algorithm and is the simplest among the JPEG DCT based algorithms. The JPEG baseline system contains a FDCT (forward discrete cosine transform), a quantizer and a Huffman encoder, where the quantization introduces data losses. Quantization and Huffman coding can make use of table look-up techniques. A progressive mode allows improving the precision of the coefficients progressively.

The DCT convert images from the spatial domain to the frequency domain and is a measure of how fast intensities of an image are changing. In themselves, DCT's do not achieve compression; all that they do is represent an image in the frequency domain. Since we expect the nightglow images to be homogeneous by regions, this could nevertheless be an advantage for compression with the Huffman coding. The main drawback of using the JPEG algorithm is its complexity which might be a heavy task for the microcontroller and take a lot of time.

e) JPEG2000

JPEG 2000 is a wavelet-based image compression standard. JPEG 2000 can operate at higher compression ratios without generating the characteristic 'blocky and blurry' artifacts of the original DCT-based JPEG standard. It also allows more sophisticated progressive download, but the required computational power is even higher than for the JPEG and thus requires more time. The JPEG2000 is a lossless compression algorithm.

f) CCSDS recommended standard for image data compression

The compression technique described in the Recommended Standard is based on discrete wavelet transform combined with a bit-plane encoder. It provides high lossless image compression, but requires a lot of calculation. The Recommended Standard differs from the JPEG2000 standard in several respects.

- it specifically targets high-rate instruments used on board of spacecraft;
- a trade-off has been performed between compression performance and complexity with particular emphasis on spacecraft applications
- the lower complexity of this recommendation supports fast and low-power hardware implementation
- it has a limited set of options, supporting its successful application without in-depth algorithm knowledge.

The major drawbacks of this compression algorithm are the fact that it is not provided as open source code and the high computational power which is required.

5.3.4.3 Header

The header indicates which image frame is stored in the long-term memory or sent to the ground station. It will include

- the absolute time when the picture has been taken with a precision of 10 minutes [TBC],
- the orientation of the satellite at the time the picture was taken with a precision of 3° (3σ) [TBC],
- the position of the satellite at the time the picture was taken with a precision of 200 km [TBC],
- the beginning and end of a frame and the compression parameters of the image [8 bits].

6 BASELINE DESIGN / ANALYSIS RECOMMENDATIONS

At the time of writing, the payload configuration is characterized by:

- a satellite at an altitude of 400 km which scans the Earth's limb with a back-looking mode, a pointing accuracy of 6.5° and a pointing stability of $0.1^\circ/\text{s}$ (hence the maximum integration time for the capturing of the image is 0.17 s)
- a measuring of the $\text{O}_2\text{A}(0-0)$ emission at 762 nm at night- and daysky (since there are not enough photons emitted at the other oxygen line)
- an optical system which comprises two lenses with an aperture of $\text{Ø}25$ mm and a focal length of 65 mm
- a SPAD-array of 128 x 128 pixels which are used to capture an area of 256 km x 256 km in a single frame.
- one ground station which communicates with the satellite and provides maximum theoretical coverage of 50 % of the Earth's atmosphere in 90 days. Thus, there will be scientific measurements every 28 orbits.

6.1 Mass and power budget of the scientific instrument

The mass distribution of the scientific instrument for the payload configuration described above is described in Table 7.

| | Mass [g] |
|-------------------|----------|
| Optics | 40 |
| Support structure | 50 |
| Electronics | 10 |
| Total | 100 |

Table 7: Mass estimates of the scientific instrument.

The power can be estimated to 33 mW for the detector during the taking of the image and for the treatment of the image with the "scientific μ -processor". Table 8 summarizes the required power and energy for the scientific instrument.

| | Power [mW] | Active time per orbit [s] | Energy [mWh] |
|------------------|------------|---------------------------|--------------|
| Detector | 100 | 6.1 | 0.11 |
| μ -processor | 100 | 1800 | 33 |
| Total | | | 33.11 |

Table 8: Power estimates of the scientific instrument.

7 CONCLUSION AND FUTURE WORK

This project allowed defining more in detail the science objectives and requirements for SwissCube and drawing a first baseline design of the scientific instrument. Several analyses provided the requirements on the physical dimensions, on the data system and on the satellite attitude, such as the pointing accuracy, the pointing stability or the coverage.

As seen in section 5.1 and subsection 5.2.4, the main challenges of SwissCube will be the SNR and the pointing stability. Both characteristics are strongly influenced by the integration time during which an image is taken. Whereas the integration time shall be as long as possible to get a good SNR, it should be small enough to reduce the constraints on the pointing stability. It might be possible to increase the integration time by following the limb image movement on the detector-array to further co-add (as the “stabilization” works in modern cameras). Another option to increase the SNR might be the combination of the output of pixels corresponding to a same altitude (horizontal binning), once the image is on ground.

Another main challenge is the design of the detector. Further analyses and tests on the characteristics of the SPADs are required to determine the feasibility of using these detectors to measure airglow emissions and the complexity introduced by this new technology. In parallel, back-up solutions, like the use of commercial CMOS-detectors, CCDs or a simple camera instead of SPADs, shall be studied and designed to assure that a scientific instrument will be ready in time for the launch in 2008.

The current payload configuration describes a preliminary design of the scientific instrument. Further analyses are required to improve its mass, dimension and power requirements by

- optimizing the detector and its control,
- optimizing the optical system of the payload,
- optimizing the data compression algorithm.